Biochemical and Biophysical Research Communications 423 (2012) 360–365

Contents lists available at SciVerse ScienceDirect

Biochemical and Biophysical Research Communications

journal homepage: www.elsevier.com/locate/ybbrc

Dynamic secondary structural changes in Ca^{2+}-saturated calmodulin upon interaction with the antagonist, W-7

Daisuke Sasakura [a,1,2], Wataru Nunomura [b,c,*,1], Yuichi Takakuwa [d]

[a] Bruker Optics K.K., Taitou 1-6-4-6F, Taitou, Tokyo 110-0016, Japan
[b] Center for Geo-Environmental Science, Graduate School of Engineering and Resource Science, Akita University, Tegata-Gakuên 1-1, Akita 010-8502, Japan
[c] Department of Life Science, Graduate School of Engineering and Resource Science, Akita University, Tegata-Gakuên 1-1, Akita 010-8502, Japan
[d] Department of Biochemistry, Tokyo Women's Medical University, Kawada 8-1, Shinjuku, Tokyo 162-8666, Japan

ARTICLE INFO

Article history:
Received 24 May 2012
Available online 1 June 2012

Keywords:
FTIR
Calcium bound calmodulin
W-7
2D-Corelation spectroscopy

ABSTRACT

Although the 3D structure of the Ca^{2+}-bound CaM (Ca^{2+}/CaM) complex with the antagonist, *N*-(6-aminohexyl)-5-chloro-1-naphthalenesulphonamide (W-7), has been resolved, the dynamic changes in Ca^{2+}/CaM structure upon interaction with W-7 are still unknown. We investigated time- and temperature-dependent dynamic changes in Ca^{2+}/CaM interaction with W-7 in physiological conditions using one- and two-dimensional Fourier-transformed infrared spectroscopy (2D-IR). We observed changes in the α-helix secondary structure of Ca^{2+}/CaM when complexed with W-7 at a molar ratio of 1:2, but not at higher molar ratios (between 1:2 and 1:5). Kinetic studies revealed that, during the initial 125 s at 25 °C, Ca^{2+}/CaM underwent formation of secondary coil and turn structures upon binding to W-7. Variations in temperature that induced significant changes in the structure of the Ca^{2+}/CaM complex failed to do so when Ca^{2+}/CaM was complexed with W-7. We concluded that W-7 induced stepwise conformational changes in Ca^{2+}/CaM that resulted in a rigidification of the complex and its inability to interact with target proteins and/or polypeptides.

1. Introduction

Calmodulin (CaM) is a ubiquitous Ca^{2+}-binding protein of 148 residues that regulates a variety of physiological processes in a Ca^{2+}-dependent manner [1–3]. The regulation is achieved through the interaction of Ca^{2+}-bound CaM (Ca^{2+}/CaM) with a large number of target enzymes [1–5]. CaM adopts an "*elongated*" structure [5–8] in which the two globular domains are connected by a highly flexible linker [9–12], both in its Ca^{2+}-bound and Ca^{2+}-free states. In contrast, Ca^{2+}/CaM complexed with target proteins adopt a compact globular shape caused by the bending of the domain linker [13–15].

A CaM antagonist, *N*-(6-aminohexyl)-5-chloro-1-naphthalenesulphonamide, W-7, has been used extensively to study the Ca^{2+}/CaM-dependent activation of various enzymes [16–18]. Distinct binding sites of W-7 have been mapped in the N-terminal and C-terminal domains of CaM (Fig. 1). Binding of W-7 induces important changes in the 3D structure of Ca^{2+}/CaM [16]. To date, studies related to structural changes in Ca^{2+}/CaM upon interaction with W-7, have been conducted in the stable state. There has not been any study of dynamic changes of Ca^{2+}/CaM upon binding to W-7.

Fourier transform infrared spectroscopy (FTIR) is a powerful tool for analyzing dynamic changes in protein structure in physiological conditions [19,20]. Second dimensional FTIR analysis as a function of time provides important information about the secondary structural changes in protein–protein and/or protein-chemical substance complexes, such as receptor-drugs. Dynamic IR spectroscopy, combined with two-dimensional (2D) correlation analysis, has been used for solving protein structure prior to and after complex formation [21–25]. This technique is a powerful tool for studying the time-dependent response of a sample as a function of an applied perturbation. Furthermore, by applying 2D correlation analysis, it is possible to identify intra- and intermolecular interactions in proteins or peptides. The power of the analysis is enhanced because of the ability to resolve overlapping spectral bands spread out over the second spectral dimension.

Abbreviations: CaM, calmodulin; Ca^{2+}/CaM, Ca^{2+}-saturated CaM; FTIR, Fourier transform infrared spectroscopy; 2D-IR, two-dimensional correlation spectroscopy; W-7, *N*-(6-aminohexyl)-5-chloro-1-naphthalenesulphonamide.

* Corresponding author. Akita University, Graduate School of Engineering and Resource Science, Center for Geo-Environmental Science and Department of Life Science, Tegata-Gakuên 1-1, Akita 010-8502, Japan. Fax: +81 18 889 2449.

E-mail address: nunomura@gipc.akita-u.ac.jp (W. Nunomura).

[1] These authors contributed equally to this work.

[2] Present address: Malvern Instruments Ltd., Kanda-Tsukasa 2-6-2F, Chiyoda, Tokyo 101-0048, Japan.

0006-291X/$ - see front matter © 2012 Elsevier Inc. All rights reserved.
http://dx.doi.org/10.1016/j.bbrc.2012.05.131

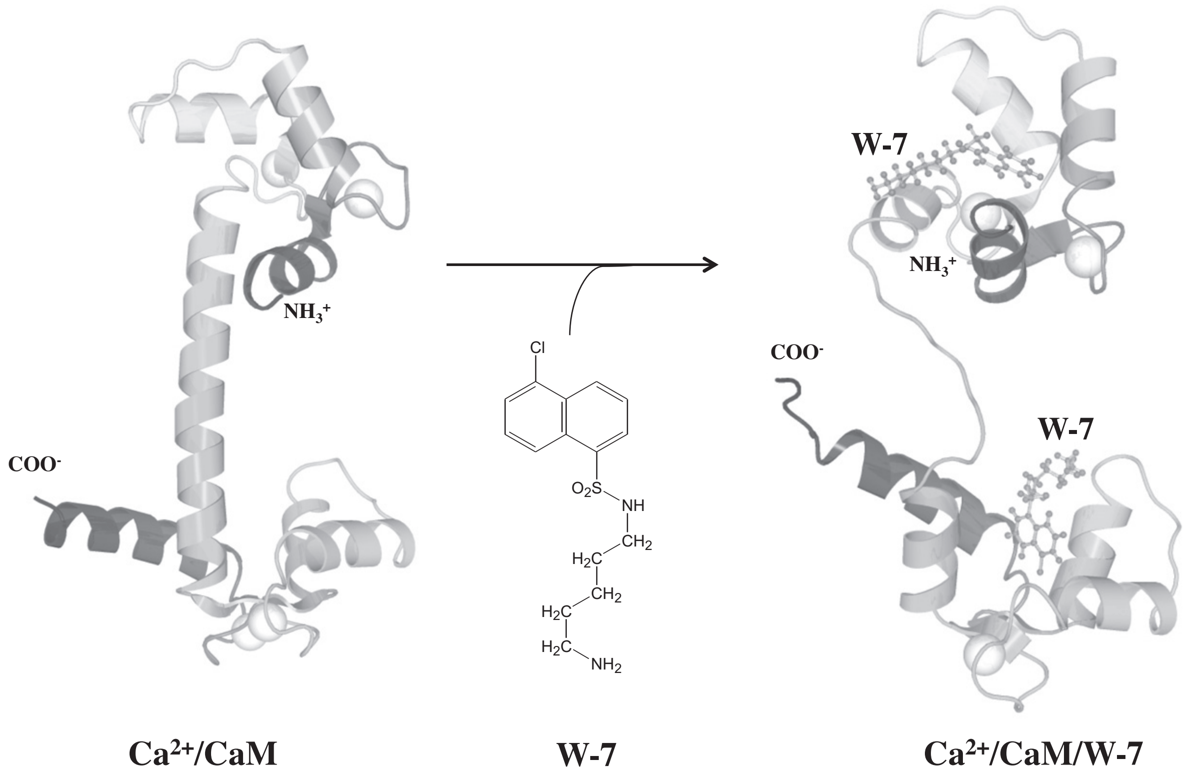

Fig. 1. 3D structure of Ca^{2+}/CaM (PDB No. 1cll) and its complex with W-7 (PDB No. 1mun).

In the present study, we confirmed by one-dimensional FTIR that the appropriate binding ratio of Ca^{2+}/CaM to W-7 was 1:2. We investigated dynamic changes in the secondary structure of Ca^{2+}/CaM upon interaction with W-7 as a function of time. During an initial period of ~125 s, changes in the secondary structure of Ca^{2+}/CaM upon binding to W-7, followed our prediction of formation of coil and turn structures. Changes in temperature induced conformational changes in Ca^{2+}/CaM but failed to do so in the context of the Ca^{2+}/CaM/W-7 complex. Together, our observations led us to conclude that W-7 induced stepwise conformational changes in Ca^{2+}/CaM leading to rigidification of Ca^{2+}/CaM and its inability to interact with its target proteins.

2. Materials and methods

CaM was purified from bovine brain by phenyl-Sepharose affinity chromatography with slight modifications, as previously described [20,26]. The purity of CaM was assessed by TOF/MS and SDS–PAGE (15% polyacrylamide gel) as previously reported [20]. CaM concentration was calculated based on the absorbance at 280 nm and an $E^{1\%}$ of 1.6 for CaM. W-7 was purchased from Sigma–Aldrich (U.S.A).

Operation of FTIR has been previously described [20]. Briefly, infrared spectra of proteins in solution, CaM or a 1:1 (molar ratio) mixture of CaM and W-7 dissolved in 50 mM Tris–HCl, pH 7.5, 0.15 M NaCl, 1 mM EDTA and 5 mM $CaCl_2$ (Buffer A), were recorded with a Tensor27 spectrometer (Bruker Optik GmbH, Ettlingen, Germany). Protein samples were prepared in a BioATR celli II (Harrick Scientific Products Inc., NY, USA), connected to a thermostat (DC30-K20, Thermo Scientific Haake Products, NH, USA).

The BioATR sample cell was used to analyze protein samples in solution. For each spectrum, a 64 scan interferogram was obtained at a single beam mode at 4 cm^{-1} resolution. Reference spectra for Buffer A alone were recorded under identical conditions. Recorded and evaluated infrared spectra were analyzed with the Opus 6.5 software (Bruker Optik GmbH, Germany). Measurements were performed between 20 °C and 90 °C at 5 °C increments. Second-derivative amide I spectra were determined using 9 smoothing points according to the Savitzky-Golay algorithms [27].

The spectra were normalized by division with the static transmission spectrum and then corrected for baseline. For each experiment, several measurements were made with a small variation in the static stress. The spectra shown here are all mean normalized spectra.

Two-dimensional correlation spectroscopy (2D-IR) of the one-dimensional FTIR spectra was implemented in MATLAB [28]. A single window over the entire time range of the experiment (0–125 s) was used. From the complete series of FTIR spectra as a function of time, the raw data of the amide I band were taken, smoothed twice by spline interpolation and a linear back-ground (1600–1700) cm^{-1} was subtracted. Next, the dynamic component of the FTIR spectra was calculated by subtraction of the static component. Since subtraction of an average static spectrum can amplify noise and introduce false peaks when the dynamic component has relatively low amplitude versus the static component [29], we used a steady-state spectrum as reference. The discrete Fourier transformation and its conjugate transformation for a given structural event pair (e.g., change at ν_1 versus change at ν_2) were calculated and summed separately. A complex number for each possible pair of wavenumbers (ν_1, ν_2) was obtained: $\Phi + \Psi i$. The real component Φ of this complex number represents the synchronous component of the correlation, the imaginary part Ψ corresponding to the asynchronous component. Real and imaginary components of $\Phi + \Psi i$, enabled to construct synchronous and asynchronous plots that were analyzed according to the rules described by Noda [21,22].

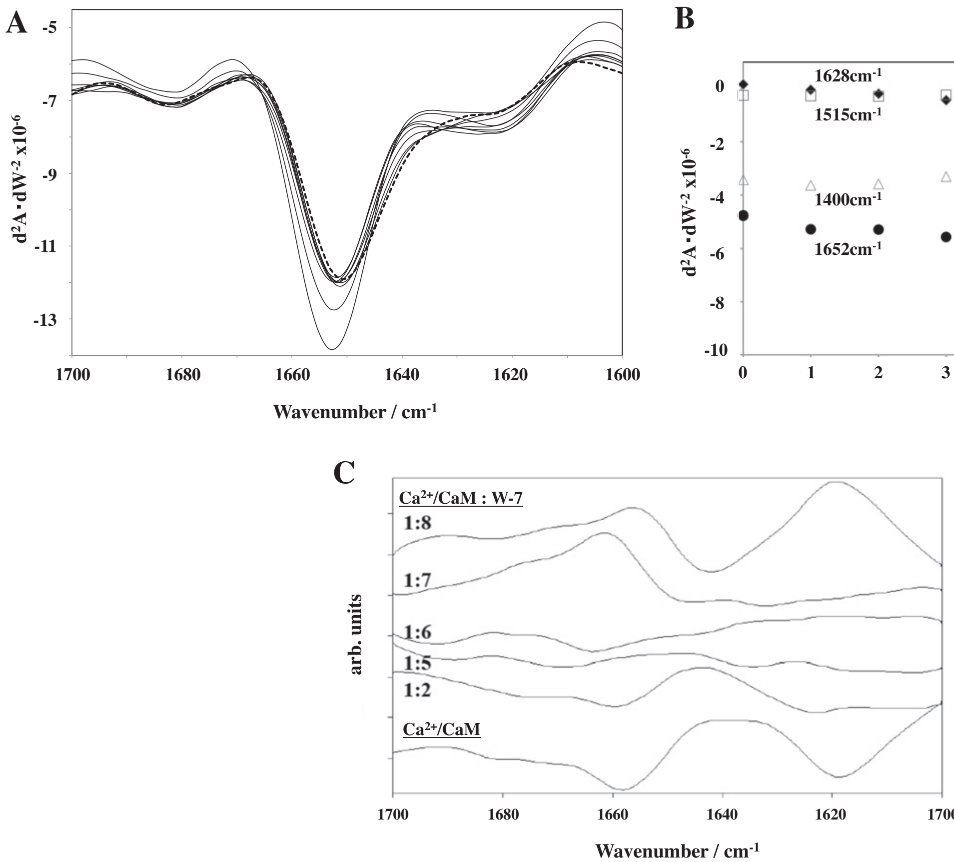

Fig. 2. Secondary derivative spectra of Ca^{2+}/CaM and its complex with W-7 at different molar ratios. The dotted and solid lines correspond to the secondary derivative spectra for Ca^{2+}/CaM and for its complex with W-7 at different Ca^{2+}/CaM:W-7 molar ratios, 1:1–1:8 (A). The d^2A/dW^2 scale is plotted on the *y*-axis where A and W represent absorbance and wavenumber, respectively. Changes in specific wavenumbers assigned to β-sheet (1628 cm^{-1}), α-helix (1652 cm^{-1}), tryptophan (1515 cm^{-1}) and aspartic acid mediating Ca^{2+} ion binding (1400 cm^{-1}) were measured as a function of molar ratios as previously described by Nara et al. [30] (B). Derivative spectra for Ca^{2+}/CaM alone and Ca^{2+}/CaM complexed with W-7 at various molar ratios (C).

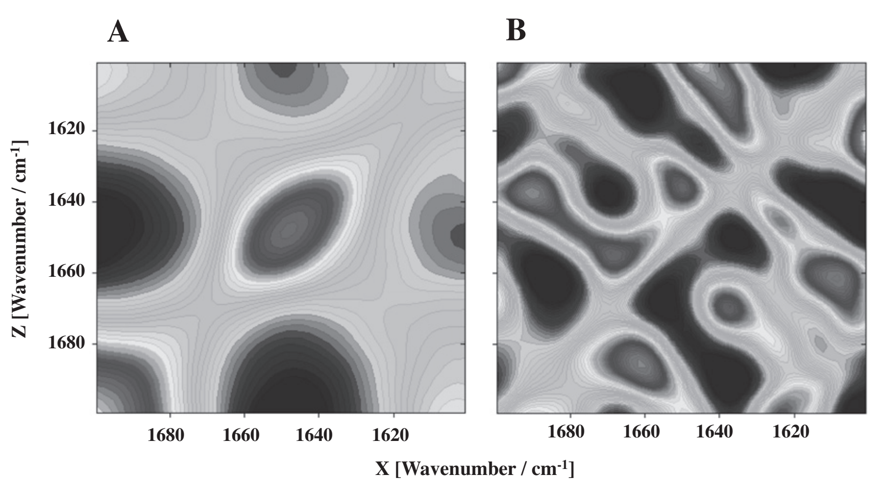

Fig. 3. 2D IR correlation spectra for Ca^{2+}/CaM binding to W-7 in the 1600 cm^{-1}–1700 cm^{-1} spectral range. (A) synchronous and (B) asynchronous profiles at 25 °C are shown.

3. Results and discussion

Secondary derivation for spectra of either Ca^{2+}/CaM alone or complexed with W-7 at different Ca^{2+}/CaM:W-7 molar ratios, i.e. 1:1–1:8, were generated (Fig. 2A). In the presence of W-7, the profiles of secondary derivation of spectra were slightly changed compared to those for Ca^{2+}/CaM alone. Marked changes were observed in the Ca^{2+}/CaM/W-7 complex at 1650–1657 cm^{-1} at molar ratios greater than 1:7. However, in contrast to the dramatic changes observed for the 1657 cm^{-1} band, a band that could be assigned to an α-helix structure, none of the others bands (and corresponding structures), 1628 cm^{-1} (β-sheet) [20], 1652 cm^{-1} (α-helix), 1515 cm^{-1} (tryptophan) and 1400 cm^{-1} (aspartic acid corresponding to a Ca^{2+} ion binding site) [30] changed significantly

Table 1
Observed IR wavenumber assignments to the secondary structure of Ca^{2+}/CaM upon binding to W-7.

Wavenumber (cm^{-1})	Assignment to secondary structure
1609	Turn
1630	Coil
1636	Coil
1650	Helix
1660	Helix
1672	Turn
1682	Turn

(Fig. 2B). Dynamic spectra were estimated from derivative spectra for Ca^{2+}/CaM alone and Ca^{2+}/CaM complexed with W-7 at various molar ratios. Dramatic changes were observed at the 1658 and 1620 cm^{-1} wavenumbers upon formation of a complex with W-7 at molar ratios greater than 1:2 (Fig. 2C).

Although the 3D structure confirmed that one molecule of Ca^{2+}/CaM bound to two molecules of W-7, calculation of the stoichiometry of binding of W-7 to CaM remains challenging. Analysis of W-7 binding to Ca^{2+}/CaM by SAXS measurements has revealed a drastic decrease in the R_g down to 17.4 ± 0.3 Å a 1:2 Ca^{2+}/CaM:W-7 ratio. These results are consistent with R_g values at various molar ratios of Ca^{2+}/CaM and Ca^{2+}/CaM/W-7 complex [17,18]. Osawa et al. have also published Guinier plots for Ca^{2+}/CaM alone and the Ca^{2+}/CaM/W-7 complex at a 1:5 Ca^{2+}/CaM:W-7 molar ratio. The R_g value for Ca^{2+}/CaM (20.3 ± 0.7 Å) presented here is also comparable to that previously reported [18]. Size exclusion chromatography experiments have indicated that W-7 binds to Ca^{2+}/CaM with a dissociation constant of 11 μM [31]. We have observed that a large excess of W-7 (ratios greater than 1:5) can result in non-specific aggregation between Ca^{2+}/CaM and W-7. Since reaching an equilibrium requires an excess of W-7 molecules compared

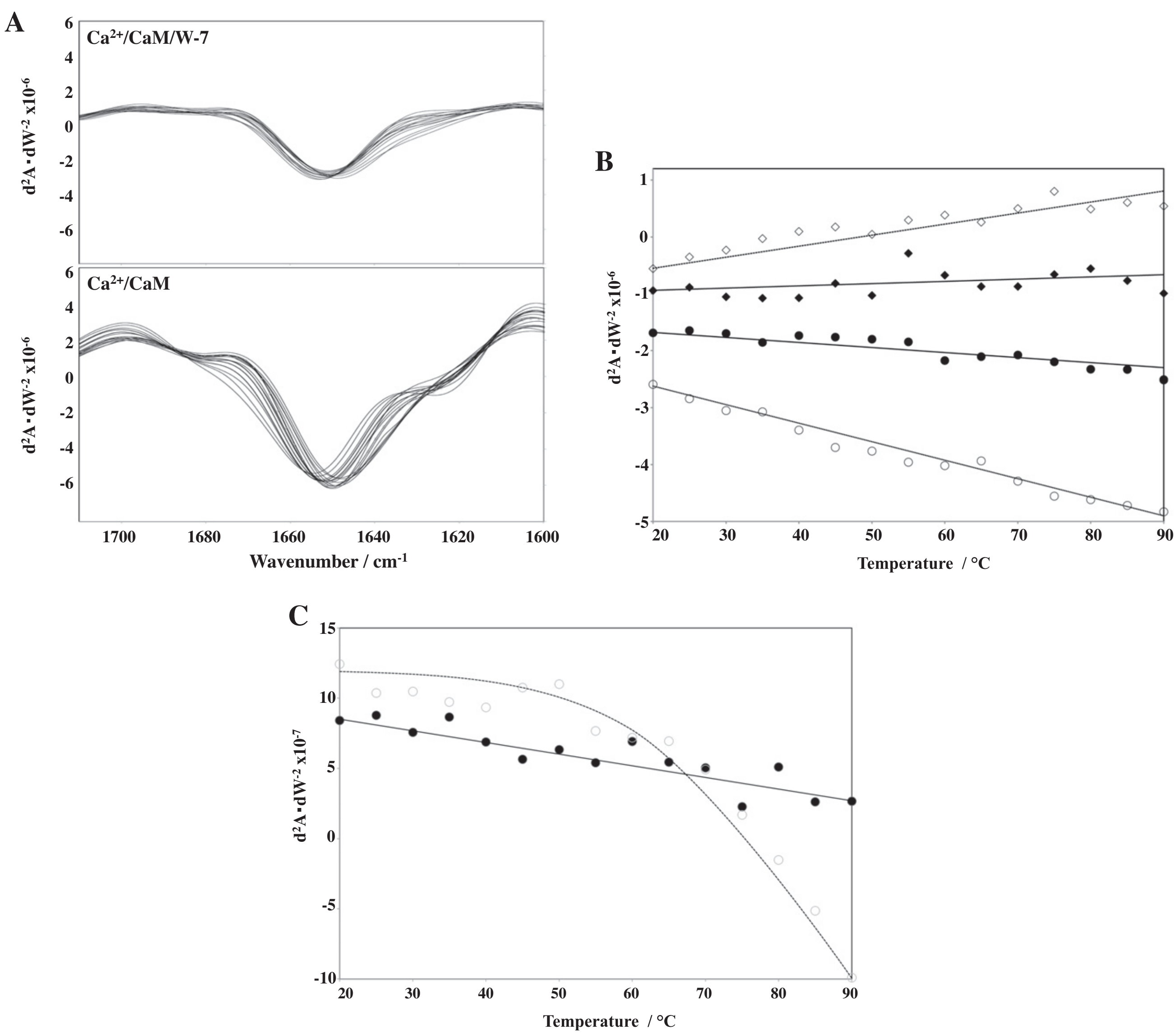

Fig. 4. Stabilization of Ca^{2+}/CaM upon W-7 binding. FT-IR measurements enable to visualize second derivative of changes in Amide I region (1700–1600 cm^{-1}). Second derivative of changes in Amide I region for Ca^{2+}/CaM (*Ca^{2+}/CaM*) and for Ca^{2+}/CaM bound to W-7 (*Ca^{2+}/CaM/W-7*) as a function of temperature at a W-7:Ca^{2+}/CaM molar ratio of 2:1 is shown (A). Changes in absorbance for specific regions of Ca^{2+}/CaM (1628 cm^{-1} for α-helix and 1652 cm^{-1} for β-sheet structure) in the presence or absence of W-7 as a function of temperature are shown in (B). Open and closed circles (1652 cm^{-1}) and squares (1628 cm^{-1}) refer to Ca^{2+}/CaM and the Ca^{2+}/CaM/W-7 complex, respectively. The same d^2A/dW^2 scale (*y* axis) is used for both 1628 and 1652 cm^{-1}, A and W representing absorbance and wavenumber, respectively. Changes in absorbance for specific regions of Ca^{2+}/CaM (1628 cm^{-1} for α-helix and 1652 cm^{-1} for β-sheet structure) as a function of temperature and in the presence or absence of W-7 are shown in (C). Open and closed circles (1672 cm^{-1}) refer to Ca^{2+}/CaM and the Ca^{2+}/CaM/W-7 complex, respectively.

to CaM due to a low binding affinity, we chose a Ca^{2+}/CaM:W-7molar ratio of 1:2 in subsequent experiments.

We then recorded 2D-IR spectra of Ca^{2+}/CaM upon binding to W-7 over the first 125 s (Fig. 3). In the C=O vibration region, the synchronous plot showed a very strong peak at the 1650 cm^{-1} band corresponding to an α-helix structure (Fig. 3A). According to the interpretation rules described by Noda [21,22], the positive crosspeak at (ν_1, ν_2) in a synchronous plot indicates that the intensities of ν_1 and ν_2 vary in the same direction. Thus, the positive crosspeak at 1650 cm^{-1} suggested that the α-helix structure had formed at a very initial stage of Ca^{2+}/CaM interaction with W-7.

The corresponding asynchronous plots in Fig. 3B indicated that the 1672 cm^{-1} band was characterized by a positive peak compared to the 1682 and 1636 cm^{-1} bands but by a negative peak when compared to the 1650 and 1630 cm^{-1} bands. Furthermore, the 1660 cm^{-1} band appeared as a positive peak compared to the 1609 cm^{-1} but as a negative a peak when compared to the 1682 cm^{-1} band. According to the interpretation rules described by Noda, in an asynchronous plot, if $\nu_1 > \nu_2$, (ν_1, ν_2) is positive, band ν_1 will vary prior to band ν_2, and if (ν_1, ν_2) is negative, band ν_1 will vary after band ν_2. Thus, the positive peak at 1672 cm^{-1} indicated that the variation of spectral intensity at 1682 cm^{-1} (*turn*) occurred earlier than that at 1636 cm^{-1} (*coil*). We also found a positive cross peak at 1672 cm^{-1} and a negative cross peak at 1650 cm^{-1} (*helix*) and 1630 cm^{-1} (*coil*). Furthermore, cross peak at 1660 cm^{-1} (*helix*) and a negative cross peak at 1609 cm^{-1} (*turn*) and 1682 cm^{-1} (*turn*) (assignment of wavenumber is shown in Table 1). We therefore predicted that secondary structure changes in Ca^{2+}/CaM upon binding to W-7 might occur according to the following order: 1609 cm^{-1} (*turn*) > 1660 cm^{-1} (*helix*) > 1682 cm^{-1} (*turn*) > 1636 cm^{-1} (*coil*) > 1672 cm^{-1} (*turn*) > 1630 cm^{-1} (*coil*). However, we cannot rule out that the coil and turn structure might form in an independent manner. As shown in Fig. 1, whereas the structure of the middle hinge region of Ca^{2+}/CaM is an helix structure in the absence of W-7, it becomes a coil structure in the context of the Ca^{2+}/CaM/W-7 complex. The two W-7 molecules bind to the N- and C-lobe of Ca^{2+}/CaM as shown in Fig. 1, this binding causing secondary structure changes in the "*hinge*" region of Ca^{2+}/CaM.

The stability of the secondary structure of Ca^{2+}/CaM as a function of temperature was increased upon W-7 binding (Fig. 4A). The bands at 1652 cm^{-1} (assigned to an α-helix structure) and at 1628 cm^{-1} (assigned to a β sheet) for Ca^{2+}/CaM changed with temperature, a phenomenon that was not observed for the Ca^{2+}/CaM/W-7 complex (Fig. 4B). Thus, although the pattern of the band at 1672 cm^{-1} (assigned to a turn structure) changed over 60 °C, only a slight change was observed for that same band for the complex (Fig. 4C). The hydrodynamic diameter of Ca^{2+}/CaM was not changed with temperature up to 55 °C, its size increasing exponentially over 60 °C, as shown by dynamic light scattering (DLS; data not shown) [20,32]. Under 55 °C, the α-helix and β-sheet secondary structures in Ca^{2+}/CaM were stabilized by W-7 binding.

In conclusion, our study, based on 2D-IR, supported that W-7 induced stepwise conformational changes in Ca^{2+}/CaM that led in turn to a stabilization of the secondary structure of Ca^{2+}/CaM (under non-aggregating conditions). Furthermore, we observed that, although the middle "*hinge*" region of CaM is a loop structure, W-7 stabilized mainly the α-helix and the turn structures but not the β-strand structures of both lobes of Ca^{2+}/CaM. Our observations led us to conclude that binding of W-7 induced a rigidification of the Ca^{2+}/CaM structure and, as a result, precluded binding to its target proteins and polypeptides.

Acknowledgments

The authors thank Dr. Philippe Gascard, Department of Pathology, University of California, San Francisco, for critical reading and editing of the manuscript before submission. The authors also thank Dr. Kohei Shiba, Sysmex Corp., Kobe, Japan for his technical assistance in performing DLS measurement.

References

[1] L.A. Jurado, P.S. Chockalingam, H.W. Jarrett, Apocalmodulin, Physiol. Rev. 79 (1999) 661–682.
[2] K.P. Hoeflich, M. Ikura, Calmodulin in action: diversity in target recognition and activation mechanisms, Cell 108 (2002) 739–742.
[3] M.J. Berridge, M.D. Bootman, H.L. Roderick, Calcium signalling: dynamics, homeostasis and remodelling, Nat. Rev. Mol. Cell Biol. 4 (2003) 517–529.
[4] J.L. Gifford, M.P. Walsh, H.J. Vogel, Structures and metal-ion-binding properties of the Ca^{2+}-binding helix-loop-helix EF-hand motifs, Biochem. J. 405 (2007) 199–221.
[5] A.P. Yamniuk, H.J. Vogel, Calmodulin's flexibility allows for promiscuity in its interactions with target proteins and peptides, Mol. Biotechnol. 27 (2004) 33–57.
[6] B.E. Finn, J. Evenas, T. Drakenberg, J.P. Waltho, E. Thulin, S. Forsén, Calcium-induced structural changes and domain autonomy in calmodulin, Nat. Struct. Biol. 2 (1995) 777–783.
[7] R.H. Kretsinger, S.E. Rudnick, L.J. Weissman, Crystal structure of calmodulin, J. Inorg. Biochem. 28 (1986) 289–302.
[8] M. Zhang, T. Tanaka, M. Ikura, Calcium-induced conformational transition revealed by the solution structure of apo calmodulin, Nat. Struct. Biol. 2 (1995) 758–767.
[9] B.A. Seaton, J.F. Head, D.M. Engelman, F.M. Richards, Calcium-induced increase in the radius of gyration and maximum dimension of calmodulin measured by small-angle X-ray scattering, Biochemistry 24 (1985) 6740–6743.
[10] D.B. Heidorn, J. Trewhella, Comparison of the crystal and solution structures of calmodulin and troponin C, Biochemistry 27 (1988) 909–915.
[11] A. Persechini, R.H. Kretsinger, The central helix of calmodulin functions as a flexible tether, J. Biol. Chem. 263 (1988) 12175–12178.
[12] G. Barbato, M. Ikura, L.E. Kay, R.W. Pastor, A. Bax, Backbone dynamics of calmodulin studied by 15N relaxation using inverse detected two-dimensional. NMR spectroscopy: the central helix is flexible, Biochemistry 31 (1992) 5269–5278.
[13] M. Ikura, G.M. Clore, A.M. Gronenborn, G. Zhu, C.B. Klee, A. Bax, Solution structure of a calmodulin-target peptide complex by multidimensional NMR, Science 256 (1992) 632–638.
[14] R. Chattopadhyaya, W.E. Meador, A.R. Means, F.A. Quiocho, Calmodulin structure refined at 1.7 A resolution, J. Mol. Biol. 1992 (228) (1992) 1177–1192.
[15] W.E. Meador, A.R. Means, F.A. Quiocho, Modulation of calmodulin plasticity in molecular recognition on the basis of x-ray structures, Science 262 (1993) 1718–1721.
[16] M. Osawa, M.B. Swindells, J. Tanikawa, T. Tanaka, T. Mase, T. Furuya, M. Ikura, Solution structure of calmodulin-W-7 complex: the basis of diversity in molecular recognition, J. Mol. Biol. 276 (1998) 165–176.
[17] M. Osawa, S. Kuwamoto, Y. Izumi, K.L. Yap, M. Ikura, T. Shibanuma, H. Yokokura, H. Hidaka, N. Matsushima, Evidence for calmodulin inter-domain compaction in solution induced by W-7 binding, FEBS Lett. 442 (1999) 173–177.
[18] N. Matsushima, N. Hayashi, Y. Jinbo, Y. Izumi, Ca^{2+}-bound calmodulin forms a compact globular structure on binding four trifluoperazine molecules in solution, Biochem. J. 347 (2000) 211–215.
[19] M. Nara, F. Yumoto, H. Kagi, M. Tanokura, Infrared spectroscopic study of the binding of divalent cations to Akazara scallop troponin C: the effect of the methylene side chain of glutamate residue, Biopolymer 89 (2008) 596–599.
[20] W. Nunomura, D. Sasakura, K. Shiba, S. Nakamura, S. Kidokoro, Y. Takakuwa, Structural stabilization of protein 4. 1R FERM domain upon binding to apo-calmodul novel insights into the biological significance of the calcium-independent binding of calmodulin to protein 4.1R, Biochem. J. 440 (2011) 367–374 (Correction, 443(1): (2012) 327).
[21] I. Noda, Two-Dimensional Infrared (2D IR) Spectroscopy: Theory and applications, Appl. Spectrosc. 44 (1990) 550–561.
[22] I. Noda, Two-dimensional correlation analysis useful for spectroscopy, chromatography, and other analytical measurements, Anal. Sci. 23 (2007) 139–146.
[23] C. Berthomieu, R. Hienerwadel, Fourier transform infrared (FTIR) spectroscopy, Photosynth. Res. 101 (2009) 157–170.
[24] P. Chys, C. Gielens, F. Meersman, FTIR 2D correlation spectroscopy of α_1 and α_2 fractions of an alkali-pretreated gelatin, Biochim. Biophys. Acta 2011 (1814) 318–325.
[25] Z. Ganim, H.S. Chung, A.W. Smith, L.P. Deflores, K.C. Jones, A. Tokmakoff, Amide I two-dimensional infrared spectroscopy of proteins, Acc. Chem. Res. 41 (2008) 432–441.
[26] W. Nunomura, Y. Takakuwa, M. Parra, J. Conboy, N. Mohandas, Ca^{2+}-dependent and Ca^{2+}-independent calmodulin binding sites in erythrocyte protein 4.1. Implications for regulation of protein 4.1 interactions with transmembrane proteins, J. Biol. Chem. 275 (2000) 6360–6367.
[27] A. Savitzky, M.J.E. Golay, Smoothing and differentiation of data by simplified least squares procedures, Anal. Chem. 36 (1964) 1627–1639.

[28] P.B. Harrington, A. Urbas, P.J. Tandler, Two-dimensional correlation analysis, Chemom. Intell. Lab. Syst. 50 (2000) 149–174.
[29] P.J. Tandler, P.B. Harrington, H. Richardson, Effects of static spectrum removal and noise on 2D-correlation spectroscopy of kinetic data, Anal. Chim. Acta 368 (1998) 45–57.
[30] M. Nara, M. Tanokura, Infrared spectroscopic study of the metal-coordination structures of calcium-binding proteins, Biochem. Biophys. Res. Commun. 369 (2008) 225–239.
[31] H. Hidaka, T. Yamaki, M. Naka, T. Tanaka, H. Hayashi, R. Kobayashi, Calcium-regulated modulator protein interacting agents inhibit smooth muscle calcium- stimulated protein kinase and ATPase, Mol. Pharmacol. 17 (1980) 66–72.
[32] K. Shiba, T. Niidome, E. Katoh, H. Xiang, L. Han, T. Mori, Y. Katayama, Polydispersity as a parameter for indicating the thermal stability of proteins by dynamic light scattering, Anal. Sci. 26 (2010) 659–663.